

# Gallium nitride technology in server and telecom applications

The promise of GaN in light of future requirements for power electronics

## Abstract

This paper discusses the benefits of e-mode GaN HEMTs in high power applications such as server power supplies and telecom infrastructure.

Compared to the next best silicon alternatives, we quantitatively show how much better systems based on GaN power devices can be. We also provide further insight into corresponding topologies, choice of magnetics, and switching frequencies to take the full benefit of the next generation of power devices.

Authored by

**Dr. Gerald Deboy**, Distinguished Engineer Power Semiconductors and System Engineering,

**Dr. Matthias Kasper**, Principal Engineer Power Operated Systems,

**Juan Sanchez**, Senior Principal Power Systems Application Engineer, all at Infineon Technologies AG

## Table of contents

<b>Abstract</b>	<b>1</b>
<b>Table of contents</b>	<b>2</b>
<b>1 Introduction</b>	<b>3</b>
<b>2 Device Concepts</b>	<b>4</b>
<b>3 Application examples</b>	<b>7</b>
3.1 Server power supplies	7
3.1.1 12 V server power supplies	8
3.1.2 48 V server power supplies	11
3.2 Power supplies for telecom infrastructure	15
3.2.1 Secondary-side GaN SG HEMTs in the LLC for ultra-high power densities	18
<b>4 Summary</b>	<b>20</b>
<b>References</b>	<b>21</b>

## 1 Introduction

The commercial availability of wide-bandgap (WBG) power semiconductors with their significantly better figures of merit raises some fundamental questions on the agenda of many customers: how much better will system solutions be, based on these wide-bandgap components in terms of density and efficiency? To what extent can silicon-based solutions follow at the potential expense of more complex topologies and control schemes?

This paper tries to answer these questions for two application fields, server power supplies and telecom infrastructure.

GaN high-electron-mobility transistors (HEMTs) as lateral power devices have an order of magnitude lower gate charge and output charge than their silicon counterparts. Combined with virtually zero reverse recovery charge, they enable hard commutation of reverse conducting devices. Thus, GaN HEMTs support simpler topologies and optimize control methods seamlessly, changing between soft- and (partial) hard switching. Even though hard commutation is acceptable for silicon-based power devices in low- and medium voltage classes, Superjunction (SJ) devices, as the prominent technology in the 600 V class, prevent any such operation due to losses and voltage overshoots.

The designer of AC-DC applications has fundamentally three choices as the next best alternatives to the use of WBG devices:

- › the use of single-ended topologies such as boost converter as a power factor correction (PFC) stage,
- › totem-pole configuration with silicon-based devices by strictly avoiding hard commutation through corresponding control methods, such as triangular current mode (TCM) operation,
- › the use of cascaded converter architecture where the voltage stress is distributed to several series-connected converter stages.

While single-ended topologies may not comply with efficiency targets, alternative solutions such as the dual boost may not reach density or cost targets. Even though cascaded solutions have demonstrated their ability to meet both efficiency and density targets [1], control efforts remain challenging and may limit the use of this concept to high-power applications only.

Hence, we see considerable value in using GaN HEMTs in relatively simple bridgeless topologies such as totem-pole. This paper hence explores the value of GaN HEMTs in comparison to the next best silicon alternatives.

## 2 Device Concepts

Server and telecom applications are dominantly using silicon-based SJ devices. Before we discuss the advantages of GaN HEMTs, we'll look into the device characteristics of both concepts.

Superjunction devices have pushed for more than a decade towards ever lower on-state resistance  $R_{DS(on)}$  [2], which in turn reduces the device capacitances and makes the devices inherently faster switching.

Figure 1 shows the output capacitance ( $C_{oss}$ ) characteristics of three subsequent generations of Superjunction transistors versus an e-mode GaN gate injection transistor (GIT) HEMT. Figure 2 shows the energy  $E_{oss}$  stored in the output capacitance  $C_{oss}$ .

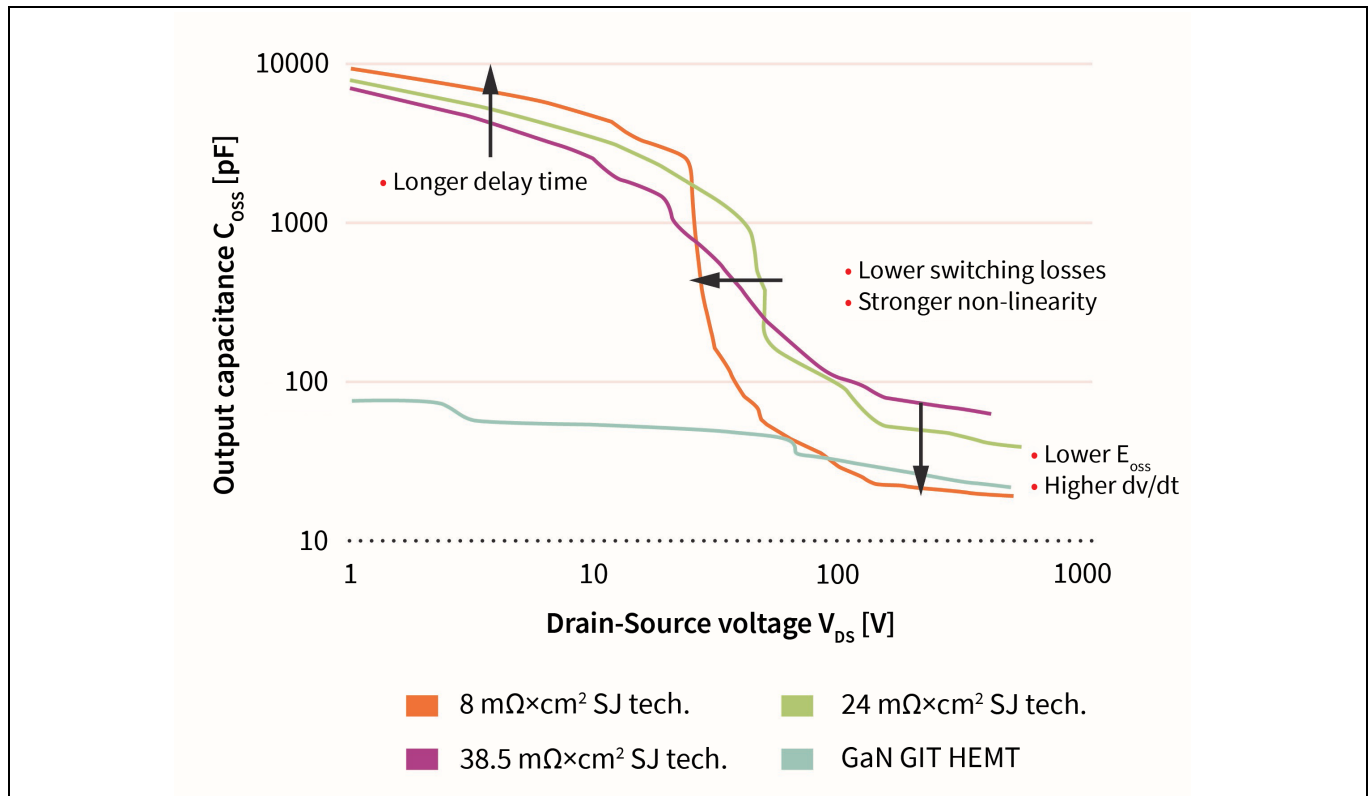


**Figure 1** Characteristic output capacitance curves of three consecutive technology nodes of Superjunction device in comparison to an e-mode GaN GIT HEMT's

Even though the output capacitance of a GaN HEMT is significantly lower in the low voltage (LV) range, the energy stored in the output capacitance is comparatively close to the values achieved by Superjunction devices.

Since this energy is dissipated as heat in every switching cycle during hard-switching transients, it is already evident from this graph that the true value of a GaN HEMT will be in half-bridge-based circuits and will be limited in single-ended topologies.

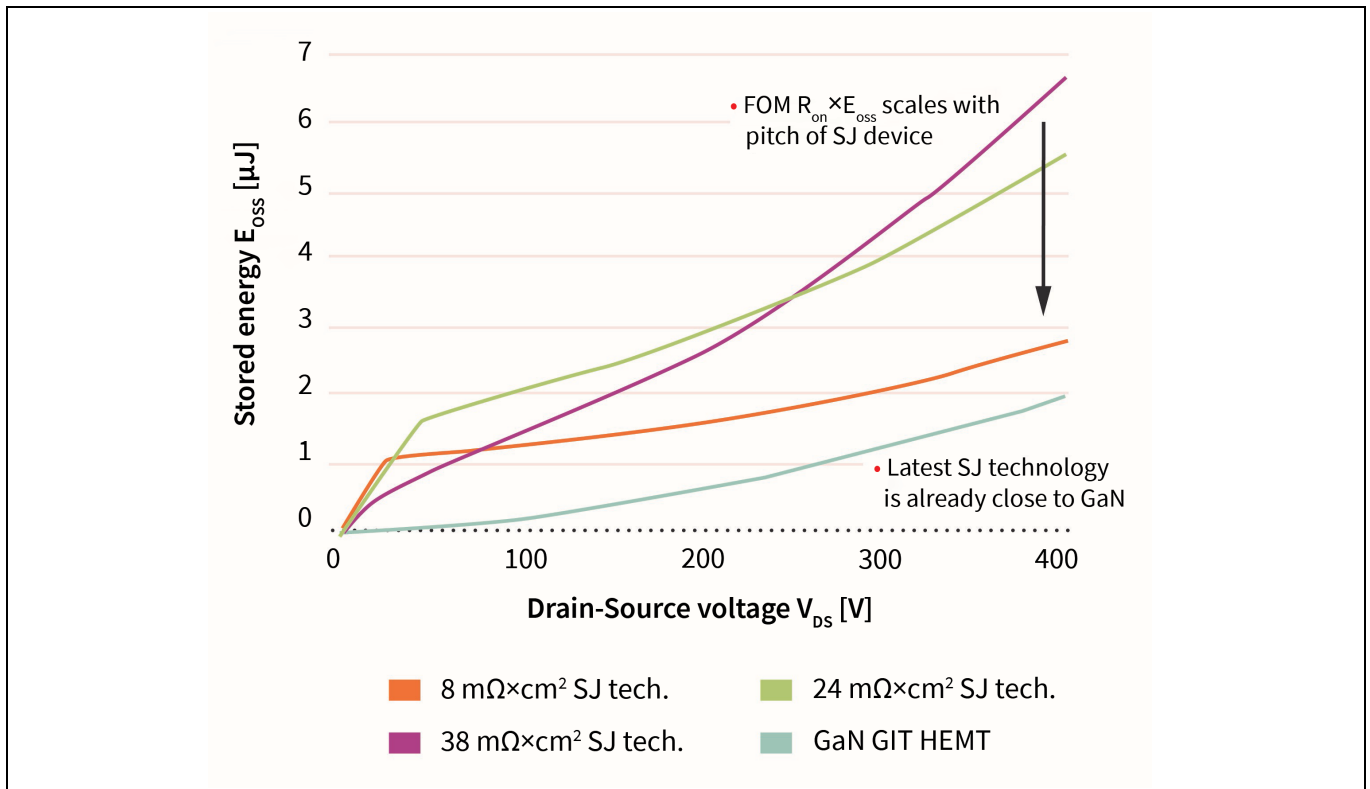


**Figure 2** The trend for the energy stored in the output capacitance across three consecutive generations of superjunction devices in comparison to CoolGaN™ GIT HEMTs

Figure 3 shows a comparison of the charge ( $Q_{oss}$ ) stored in the output capacitance as one of the key parameters for soft-switching transitions.

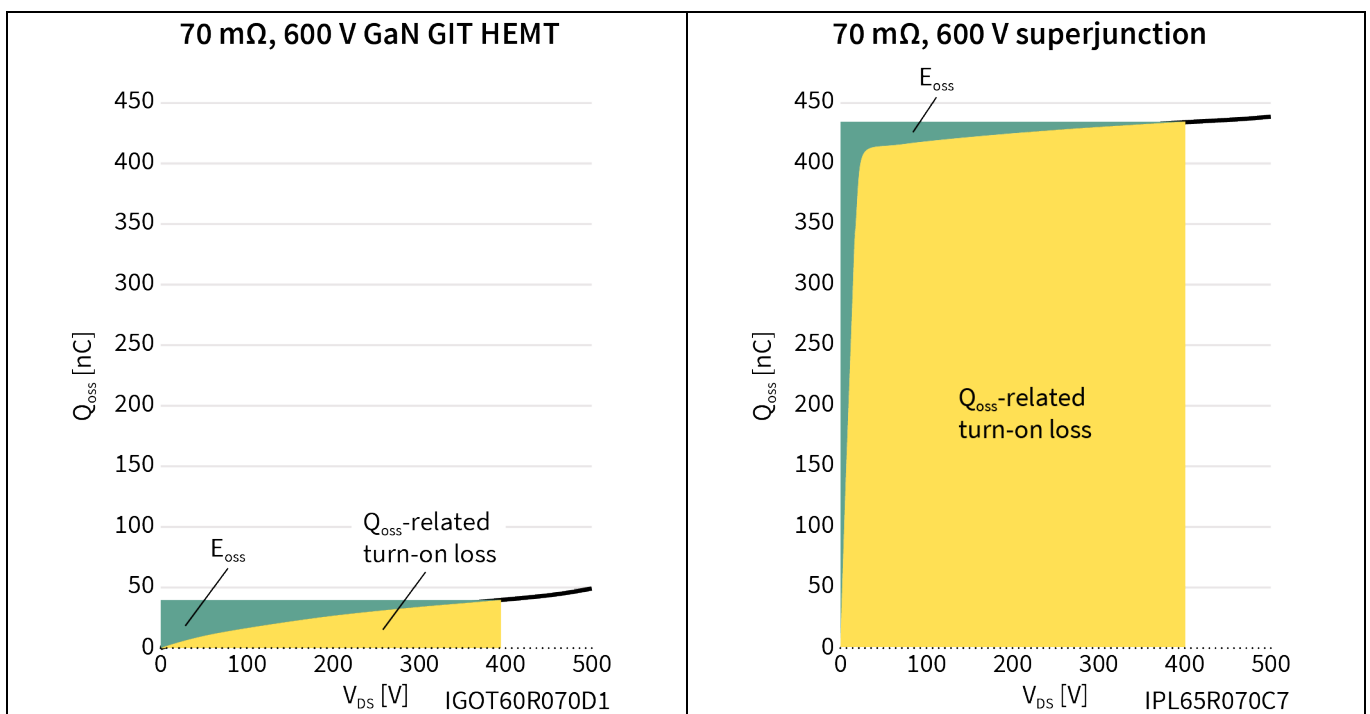


**Figure 3** Comparison of  $Q_{oss}$  versus voltage for an e-mode CoolGaN™ GIT HEMT (left) to CoolMOS™ C7 SJ MOSFET (right)

The areas colored in yellow represent the  $Q_{OSS}$ -related losses at turn-on. This is the contribution of charge flowing from the device previously conducting into the device turning-on while operating in linear mode at DC link voltage level. The green area is the amount of energy stored in the output capacitance of the device previously blocking. This energy will be dissipated as Joule loss inside the device by opening the channel and having the electron current discharge the output capacitance. In a hard commutation event with the high-side device conducting on its body diode, the yellow-colored area represents the losses associated with the high-side device. The green area represents the losses associated with the low-side device turning on. The sum of both areas indicates the total losses.

Whereas in single-ended topologies the  $E_{OSS}$  parameter governs loss mechanisms, in half-bridge (HB)-based circuits, the charge stored in the output capacitance  $Q_{OSS}$  [3] and the reverse recovery charge  $Q_{rr}$  determine the losses.

The GaN technology is a prime candidate for hard commutation with its factor 10 lower  $Q_{OSS}$  charge and its very balanced loss contributions from  $E_{OSS}$  and  $Q_{OSS}$ . While superjunction devices are optimized for an extremely low  $E_{OSS}$  figure of merit (FOM), GaN GIT HEMTs offer a much more favorable  $Q_{OSS}$  FOM, with the first generation being already one order of magnitude better than their silicon counterparts.

In the class of 100 V-rated devices,  $Q_{rr}$  and  $Q_{OSS}$  contributions are typically in the same order of magnitude for modern shielded-gate power transistors. The GaN technology clearly shows significant advantages in both parameters lowering half-bridge commutation losses to less than one-fifth of its silicon counterpart. Also, the gate charge is lower by more than factor 5, which are perfect pre-requisites for high-frequency operation.

Together with the ultra-low gate charge of GaN (cf. Figure 4), CoolGaN™ technology is the preferred choice for soft-switched topologies like the LLC topology that operate at high frequencies.

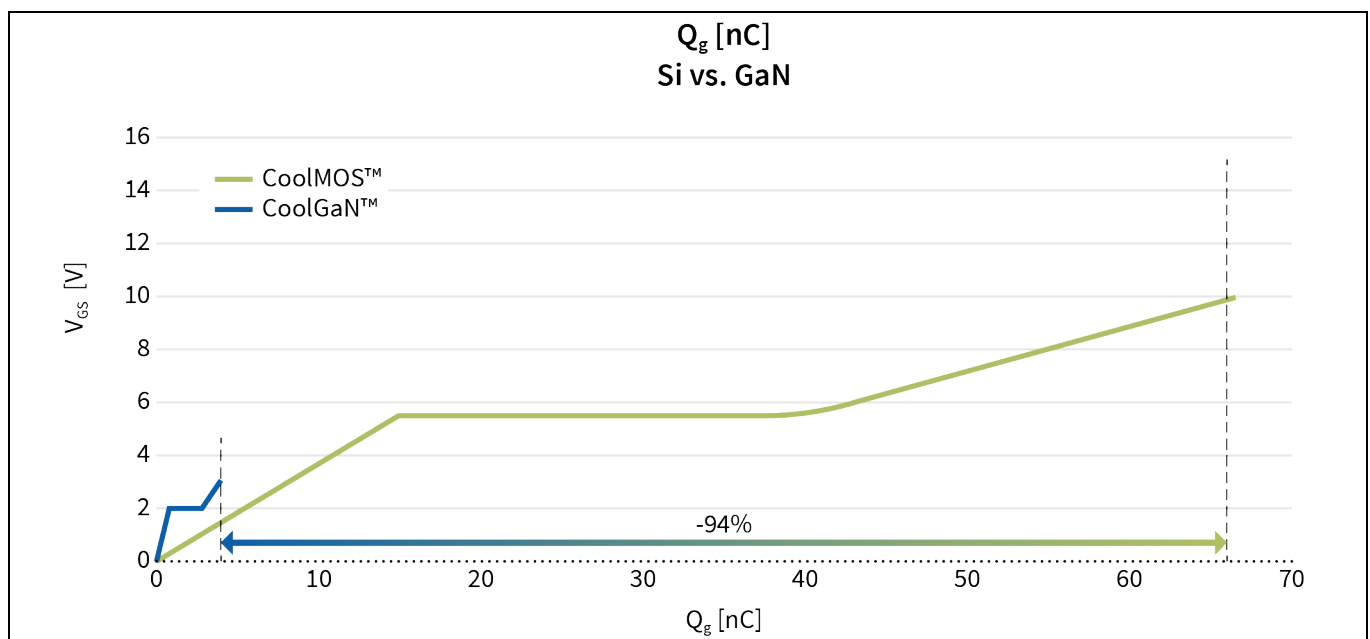


**Figure 4** Gate charge for silicon and GaN technologies

### 3 Application examples

#### 3.1 Server power supplies

The emergence of cloud-based internet services, artificial intelligence, and cryptocurrency has initiated a strong growth of processing power in data centers worldwide. Since the data centers also face rising electricity and real estate prices, there is a clear trend towards highly efficient and compact server supplies. These new power supplies not only lead to a lower power consumption of the server but also to a lower heat dissipation reducing secondary costs such as the cooling of the servers.

The best way to combine high efficiency with high power density in state-of-the-art server power supplies and telecom rectifiers is to use a bridgeless PFC stage such as a totem pole and a resonant high-voltage (HV) DC-DC stage, such as an LLC converter with full-bridge (FB) or center-tapped synchronous rectification on the secondary side (see Figure 5).

The bridgeless PFC stage consists of:

- › A high-frequency path (S1 and S2 devices), where only WBG devices can be used because they can survive the continuous operation in hard commutation typical of this topology [3].
- › A low-frequency bridge leg (S3 and S4 devices), where Si-based SJ devices with very low  $R_{DS(on)}$  represent the ideal choice.

Si SJ devices like CoolMOS™ can be used in the high switching frequency section of the totem-pole PFC only when triangular current mode (TCM) control is applied with a variable switching frequency, like in Figure 5. Higher components count and control complexity make this topology less convenient compared to the WBG-based CCM.

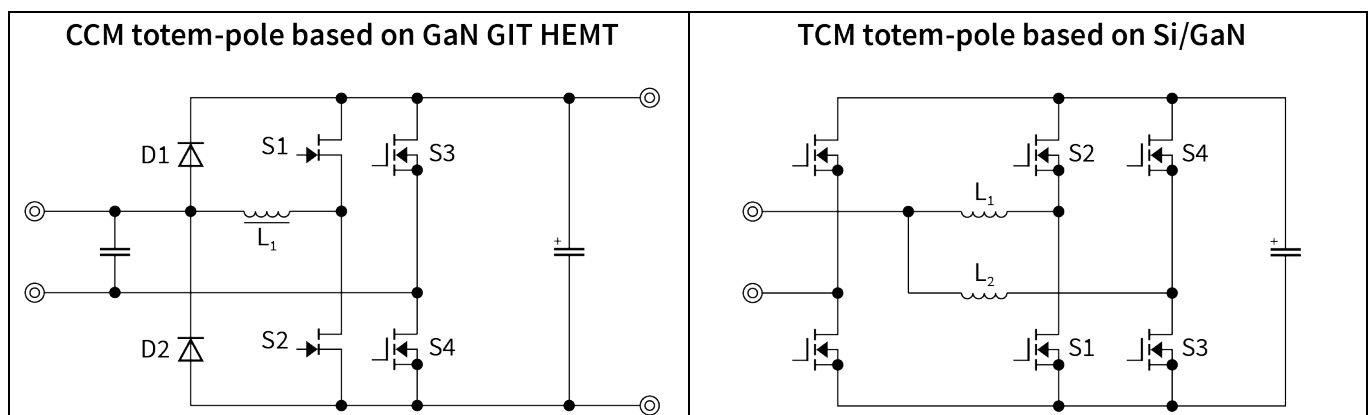


**Figure 5** CCM totem pole based on high voltage GaN GIT HEMT technologies (left) and TCM totem pole based on Si/GaN technologies (right)

Typically, state-of-the-art high-efficiency power supplies are comprised of a bridgeless or semi-bridgeless PFC stage such as a totem-pole stage and a resonant DC-DC stage such as an LLC converter (see Figure 6). For an output voltage of 12 V, a center-tapped transformer is typically used, while for 48 V systems, a full bridge rectification is considered.

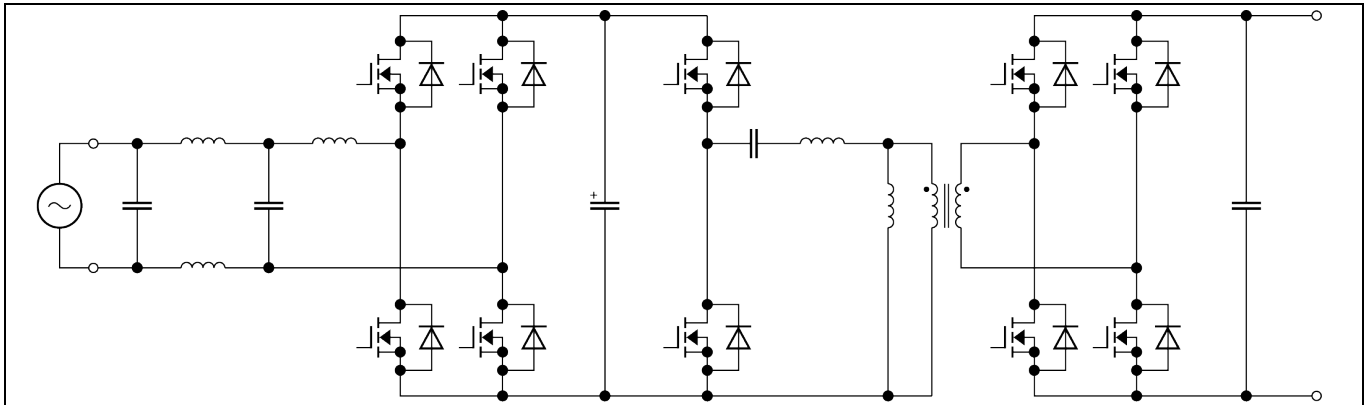


**Figure 6** Server supply comprising a totem pole AC-DC rectifier with one high frequency and one low frequency bridge leg and an LLC DC-DC converter with a full-bridge rectifier

Table 1 shows the specifications for a server power supply used as a basis for our optimization strategy.

**Table 1** Specifications for server supplies

Parameter	Variable	Value
Input voltage	$V_{in}$	180 V – 277
Output voltage	$V_{out}$	12 V / 48 V
Rated power	$P_{out}$	3 kW
Hold-up time	$T_{hold}$	10 ms

### 3.1.1 12 V server power supplies

Currently, a majority of data center operators are running their motherboards on 12 V DC input. In the legacy architecture, uninterruptible power supplies (UPS) will provide backup power to two independent AC distribution schemes throughout the data center. In a classic server board, two AC-DC power supplies provide redundancy to each other, each power supply being sufficient to cover the full power demand of the attached load.

The need for lower operational cost (OPEX) and more payload per rack to save on capital expenditure (CAPEX) will drive two major transitions: first, local energy storage on rack level to cut out the UPS from the power flow; second, the transition from server-based power supplies to rack-based power supplies to reduce redundancy from 1+1 to n+1, thus saving cost. Both trends favor higher output power in a given form factor. Hence, the focus of this paper is to analyze the benefits of GaN HEMTs towards power density.

A bridgeless topology is used (in this case, the totem-pole configuration) both for silicon switches and GaN GIT HEMTs. Using silicon devices mandates operation in triangular current mode (TCM) at all times, which results in a more complex control scheme with varying switching frequency and larger current ripples. In contrast, different modulation schemes can be selected for GaN GIT HEMTs. The capability to operate the GaN switches in both hard- and soft-switching enables the designer to run the



totem pole in continuous conduction mode (CCM), triangular conduction mode (TCM), or optimal frequency modulation (OFM). The OFM is a seamless transition between hard- and soft-switching over a grid period depending on the power level and/or grid voltage [4].

Figure 7 shows the optimization results for a silicon totem pole rectifier stage (including the EMI filter) operating in TCM and a GaN totem pole stage using TCM or CCM. Both systems are optimized to deliver peak efficiency at 50 percent of the rated power and evaluated at nominal AC input voltages. The comparison includes the volume of the power electronics, the PCB, and the additional air between the components. Excluded are the case and control/auxiliary electronics

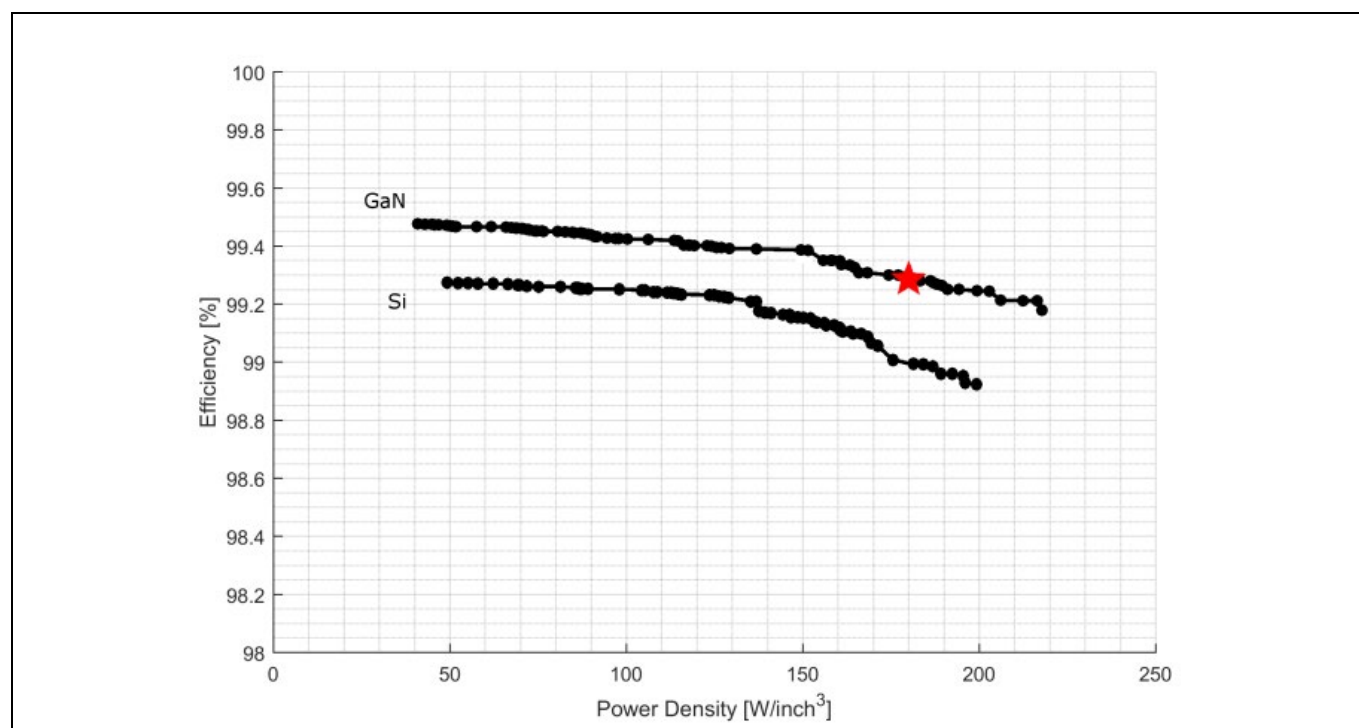


**Figure 7 Optimization result for the totem pole PFC stage, including EMI filter, comparing system efficiency versus density for both GaN- or Si-based power devices, respectively**

The results clearly indicate the higher performance of the GaN-based designs, especially towards higher power density. An analysis of the designs using GaN transistors reveals that the TCM modulation offers a benefit compared to CCM, specifically in the region of highest power density.

Similarly, the LLC stage has been optimized for Si and GaN semiconductors. The results are shown in Figure 8. As can be seen, GaN provides a simultaneous improvement of efficiency and power density.

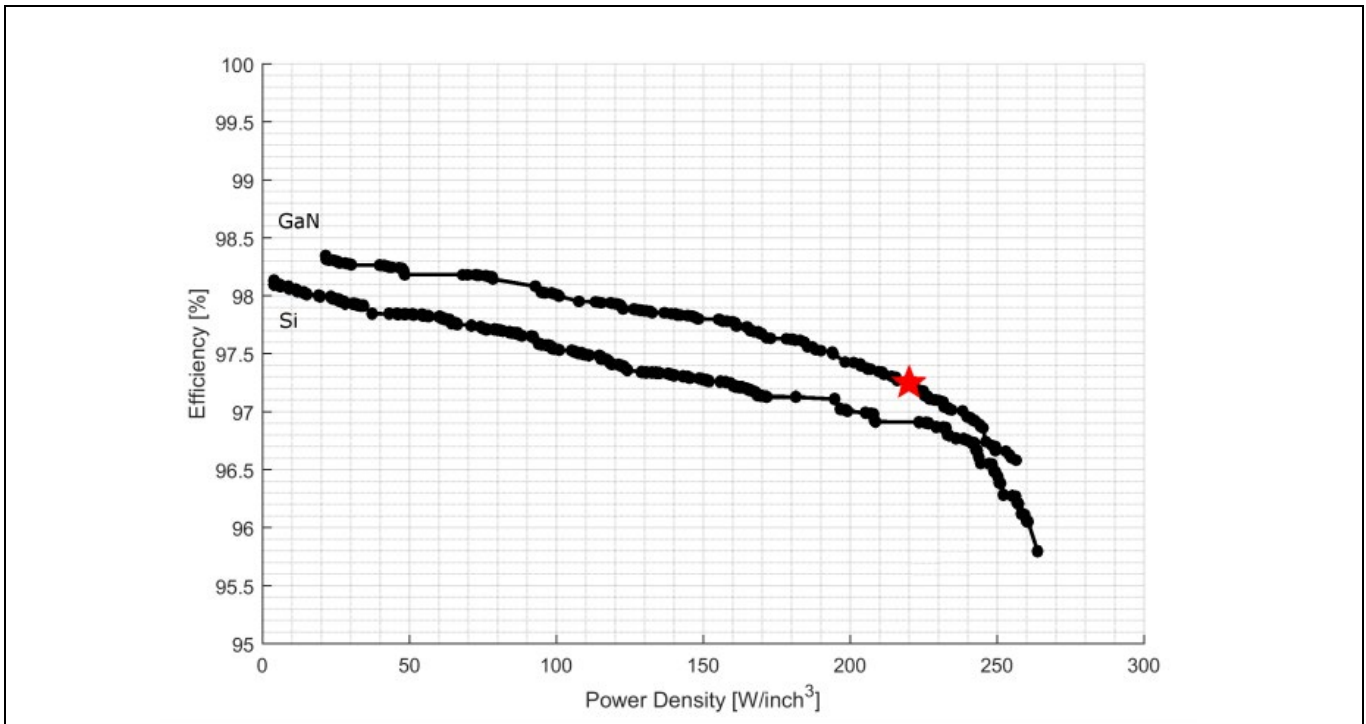


**Figure 8** Optimization results for the LLC stage showing efficiency vs. power density both for silicon and GaN-based devices

Finally, the optimization results of the entire systems are shown in Figure 9. The results include all power electronic components, auxiliary electronics, PCB, and 20 percent of additional volume being added to account for a non-ideal placement of the components. The connectors and the casing with standoff are not included.

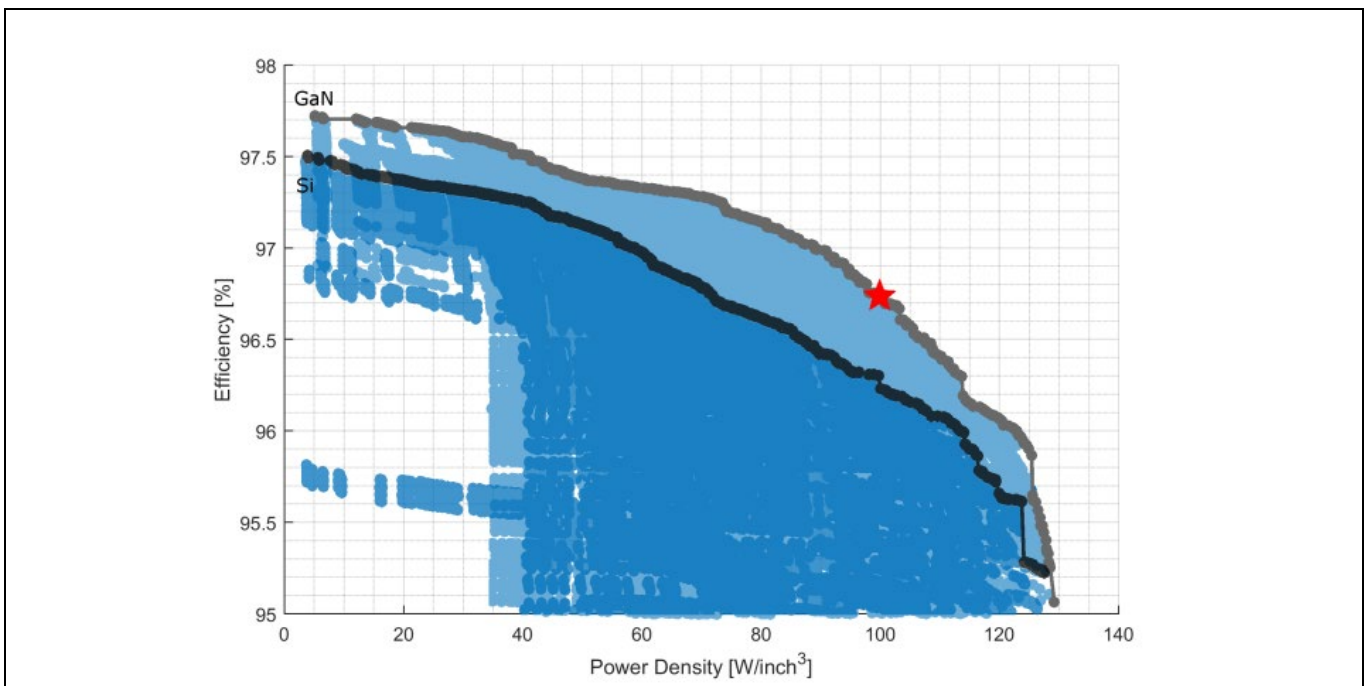


**Figure 9** Optimization results of the entire 12 V server power supply showing efficiency versus density both for GaN- or Si-based power semiconductor devices

The result clearly indicates a path to handle 3 kW in a given form factor such as the 68x41x184 mm<sup>3</sup> flex slot size, thus nearly doubling the output power in this box size. Compared to off-the-shelf solutions delivering 1600 W in this form factor, we not only nearly double the power but also increase efficiency on average by 4 percent without increasing dissipated heat within the power supply (see Figure 10).

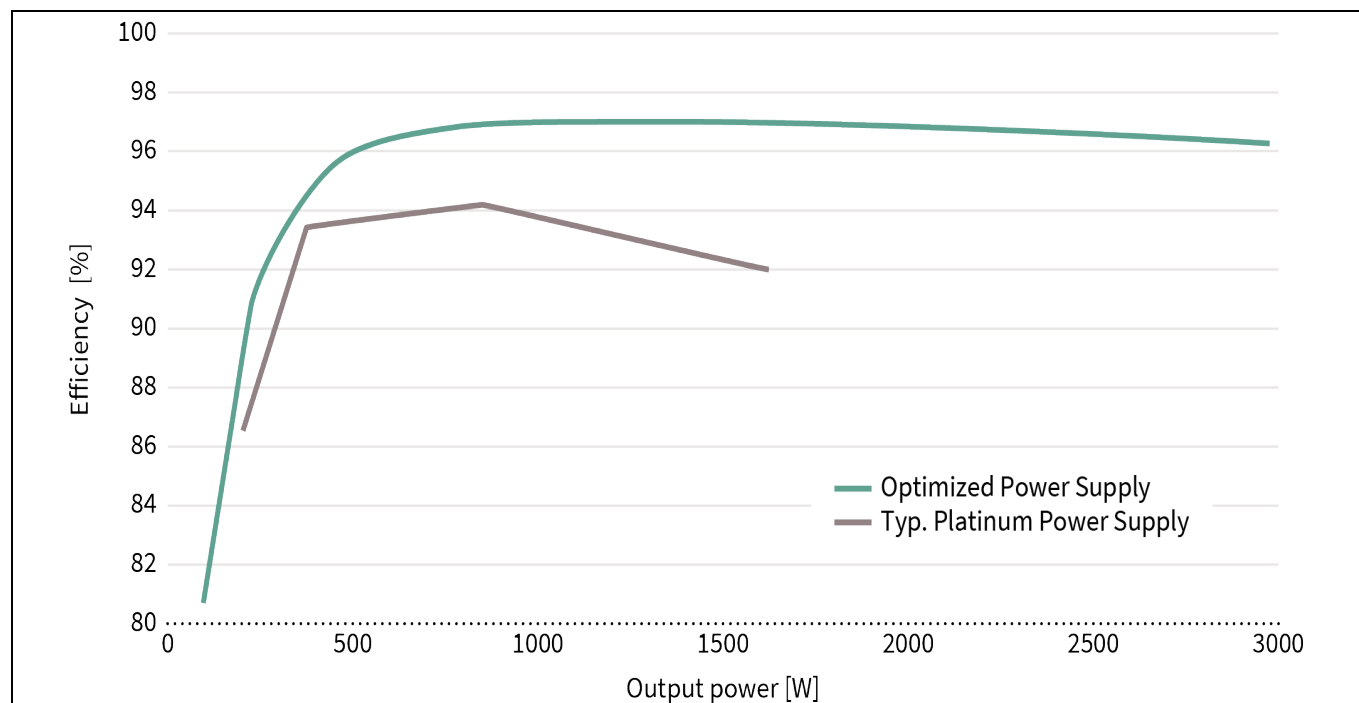


**Figure 10** Comparison of the efficiency curve of the high-density GaN server design versus a state-of-the-art Si-based power supply

### 3.1.2 48 V server power supplies

The emerging use of artificial intelligence (AI) in computer science and the training of the corresponding neural networks has shifted the computational architectures from pure CPU-based servers to more specialized platforms with a very high degree of parallel data processing (e.g., by employing GPUs).

As a result of this trend, the power consumption per rack has now roughly tripled, pushing the power per rack to 20 kW and above. This power would lead to substantial losses within classic 12 V distribution rails. As a solution, power distribution within the rack on 48 V level instead of 12 V will be more widespread in the future. Since the 48 V server supplies mainly target applications being optimized for the total cost of ownership (TCO), the performance of GaN power devices in these systems is explicitly evaluated from an efficiency perspective.

As a basis for the comparison, an industrial 48 V Si power supply with  $P_{\text{rat}} = 3 \text{ kW}$  is taken as a reference. This power supply features a peak efficiency of 97.1 percent at half of the rated power and a power density of around 33 W/inch<sup>3</sup>. As the first improvement step, the AC-DC stage can be changed into a totem pole rectifier with one high-frequency bridge leg. This is enabled by using GaN switches ( $R_{\text{DS(on) } 25, \text{ max}} = 70 \text{ m}\Omega$ ) in the high-frequency bridge leg and Superjunction MOSFETs with very low on-

state resistance in the low-frequency bridge leg. As addressed before, GaN GIT HEMTs offer a choice of different modulation schemes.

The Pareto-front for continuous conduction mode (CCM) operation at nominal operating voltages ( $V_{in} = 230\text{ V}$ ,  $V_{out} = 48\text{ V}$ ) and 50 percent power level is shown in Figure 11.

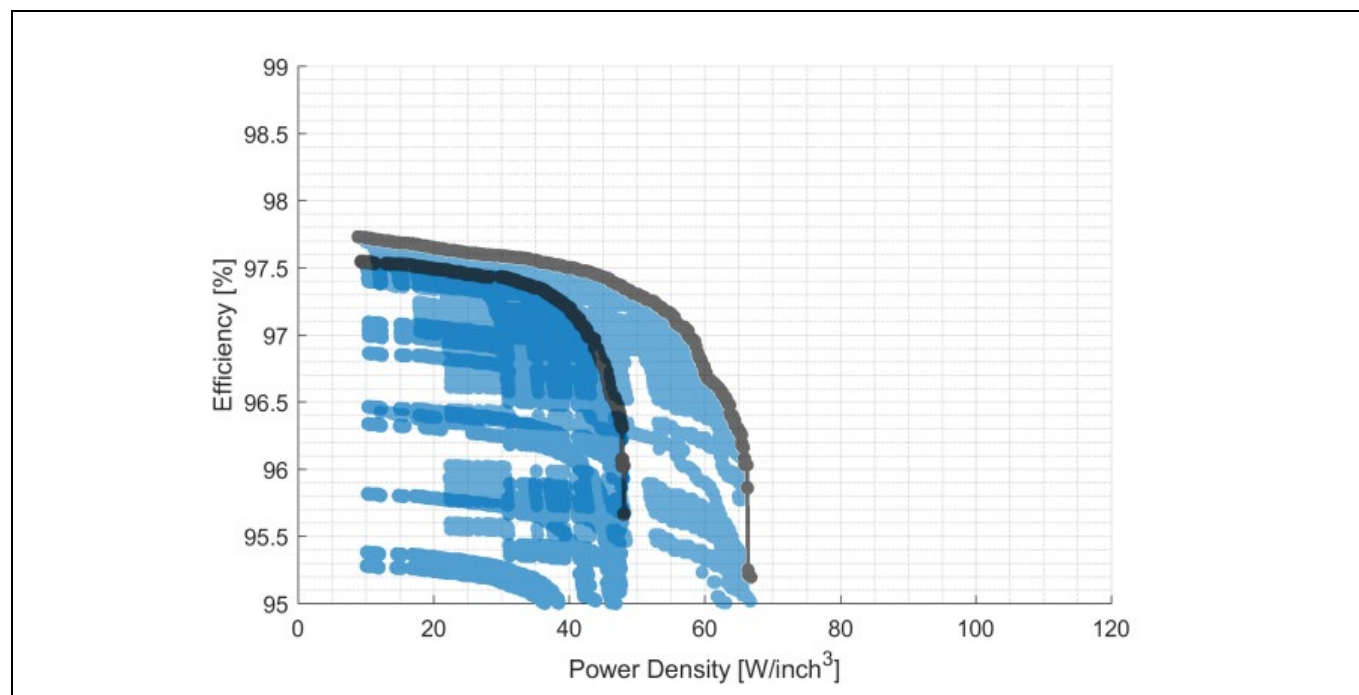


**Figure 11** Pareto-front of the state-of-art 48 V power supply at 50% load and nominal operating voltage. The performance improvement offered by interleaving two GaN high-frequency bridge-legs is overlaid.

As a second step of improving the efficiency of the AC-DC stage, several possibilities exist:

- › Using two interleaved high-frequency bridge-legs in the totem pole
- › Increasing the chip area of the high-frequency and low-frequency switches
- › Operating the totem pole in TCM

A cost analysis of the different options reveals that the most cost-effective performance improvement can be achieved by interleaving two high-frequency (HF) bridge legs using CCM control. This cuts the average current in each HF bridge leg by a factor of 2, which has two major benefits:

- › The reduced RMS current significantly lowers the conduction losses in each high-frequency branch (i.e., inductor and GaN switches).
- › Natural zero-voltage switching (ZVS) can be achieved more easily when the high-frequency current ripple (peak-peak) is larger than twice the average current, thereby reducing the switching losses.

The performance improvement is shown in Figure 11 by the overlaid opaque Pareto front.

The introduction of triangular current mode (TCM) to achieve ZVS over the whole grid period would allow a larger chip area to reduce conduction losses further. However, this is a rather costly implementation. The additional chip area and the optimization of the boost inductors for larger ripple currents with thin strands add significant cost and control complexity with an improvement potential of only around 0.1 percent at the considered level of power density. Hence, CCM control is the option of choice for efficiency and cost-driven converter designs.

In the LLC stage, there are also several improvement options. Similarly, the optimization flow is based on an industrial design using 31 mΩ fast body-diode-type Superjunction devices at a relatively low switching frequency.

As a first measure, the primary side half-bridge is equipped with 42 mΩ GaN switches. The system efficiency can be increased by around 0.3 percent by optimizing the resonant tank with one order of magnitude lower  $Q_{oss}$  charge on the switches, including adjustments of the resonant frequency and the magnetizing inductance.

On top of this, efficiency can be further improved by another 0.3 percent by changing the transformer setup to a matrix structure using two cores with series-connected primary windings and parallel-connected secondary side windings. This approach offers several advantages for the conversion efficiency:

- › The high output current of the single transformer configuration is split among the two outputs. Under the assumption that both configurations have comparable termination resistances, the total termination losses can be significantly lowered with the matrix transformer setup.
- › Due to lower currents in each transformer, the electrical fields that cause proximity effect losses are also reduced.
- › The use of two synchronous rectification (SR) stages leads to a spatial distribution of the losses of the synchronous rectification MOSFETs, which is beneficial, especially from a thermal perspective.

The input series/output parallel connection of the matrix transformer setup is inherently stable as it guarantees equal splitting of the primary voltage among the series-connected primary terminals and equal output current splitting among the secondary terminals of the transformers. Caution has to be taken to reduce the leakage inductance of each transformer such that it does not affect the resonance behavior of the LLC. The total systems cost will only marginally increase through this step.

As a further measure for performance improvements, the secondary side of the transformers can be changed from center-tapped into full-bridge rectification circuits. On the one hand, this leads to a better copper utilization in the transformers, and on the other allows to use synchronous rectification MOSFETs with a lower voltage rating and thus with a better FOM. With this configuration, the transformer and synchronous rectification losses can be further reduced, but at the expense of increased system cost



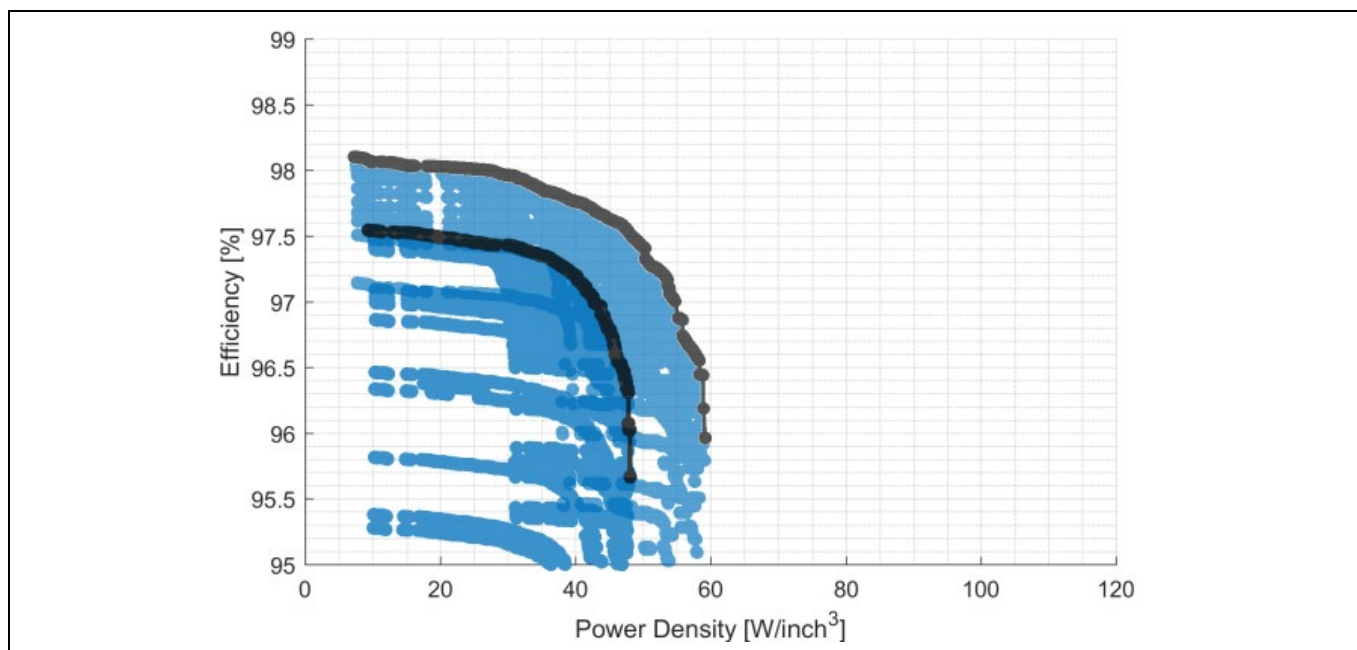


**Figure 12** Performance improvements of the 48 V server supply provided by utilizing 42 mΩ GaN as primary switches in the LLC and a matrix transformer configuration.

By combining the most cost-effective performance improvement options of both PFC (i.e., two interleaved high-frequency bridge legs with 70 mΩ GaN GIT HEMTs in CCM operation) and LLC stage (i.e., 42 mΩ GaN GIT HEMTs on the primary side and matrix transformer configuration), the total system peak efficiency can be increased by 0.8 to 0.9 percent to a level of around 98.2 to 98.3 percent. Using the full potential of all available performance improvement methods allows the entire system's efficiency to increase up to 98.5 percent, giving a power density of around 30 to 35 W/inch<sup>3</sup>.

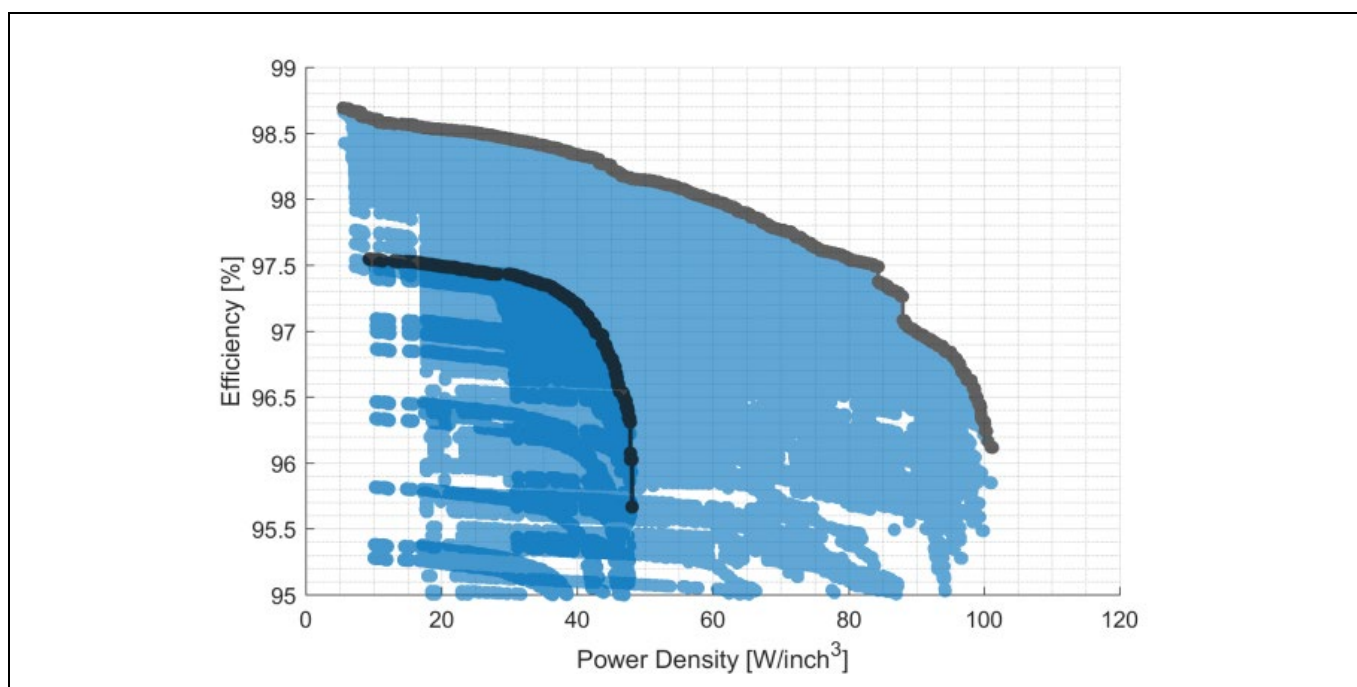


**Figure 13** Achievable Pareto-front of the entire 48 V server power supply with all PFC and LLC improvement options incorporated.

## 3.2 Power supplies for telecom infrastructure

The rapid growth of cloud-based internet services does not only affect the development of data centers but impacts the telecom infrastructure similarly. Due to increasing data traffic and the demand for higher bandwidth, telecom base stations as the ultimate link between the mobile world and hyper-scale datacenters have gained significant importance. As existing telecom sites may serve multiple antennas within the roll-out of 5G, power distribution and overall power consumption move more and more into focus.

Even though the 380 V DC distribution in telecom applications has gained popularity in recent years, the majority of telecom equipment is still powered by 48 V, in most cases referred to negative potential to inhibit corrosion. In contrast to the server power supplies, addressed in the previous chapters with a fixed output voltage, the telecom power supplies typically have an output voltage range of 40 V to 60 V and typically use no ORing MOSFETs for hot-plug capability (see Table 2).

**Table 2 Typical specifications of a telecom rectifier for macro base stations**

Parameter	Variable	Value
Input voltage	$V_{in}$	85 – 277 V <sub>AC</sub> Nominal value: 230 V <sub>AC</sub>
Output voltage	$V_{out}$	42 – 58 VDC Nominal value: 53.5 V <sub>DC</sub>
Rated power	$P_{out}$	3 kW

Another difference exists in the load profile, such that telecom power supplies operate most of the time between 30 percent and 50 percent of the rated power. In contrast, hyper-scale server supplies operate typically in the range of 50 percent to 70 percent of the rated power. This leads to different optimization targets emphasizing efficiency in the 30 percent to 50 percent load range.

In the following, the highest achievable performance with GaN HEMTs in a 3 kW telecom power supply is shown in comparison to the best Si solution. The selected topologies are the same as for the server supplies and consist of a totem pole PFC, which is either operated in CCM with GaN GIT HEMTs or in TCM with Si MOSFETs, followed by an LLC DC-DC converter.

To compare GaN GIT HEMTs and the best alternative Si solution, both systems are optimized employing a multi-objective optimization for 50 percent of the rated power and evaluated at an input voltage of 230 V and an output voltage of 48 V.

In the GaN-based designs, all high voltage switches are GaN GIT HEMTs, except for the low-frequency totem-pole return-path switches, which are in both cases 17 mΩ C7 MOSFETs (IPZ60R017C7). The low voltage switches for the secondary side of the LLC, which is a full-bridge rectifier, are in both cases 80 V OptiMOS™ 5 MOSFETs (BSC030N08NS5), with up to three devices in parallel. In order to have a fair system comparison between the two 600V device technologies, without treating one technology preferentially due to a more extensive portfolio of  $R_{DS(on)}$  values, only 70 mΩ devices are considered for the high voltage switches, i.e., CoolGaN™ (IGT60R070D1) and CoolMOS™ CFD7 (IPW60R070CFD7).

As an optimization parameter, the devices can be paralleled up to three devices, thus creating effective  $R_{DS(on)}$  values of 70 m $\Omega$ , 42 m $\Omega$ , and 23 m $\Omega$ .

Additional parameters varied during the optimization are similar to those described in the server section of this document. These include, but are not limited to, e.g., the number of HF legs in the PFC, the number of parallel PFC and LLC stages, the number of transformers connected in a matrix configuration, and switching frequencies.

The optimization results are shown in Figure 14, visualizing the achievable performance gain of CoolGaN™ GIT HEMTs in a 3 kW telecom power supply compared to the best Si solutions, which is consistently between 0.1 percent and 0.3 percent. However, the graphs do not reflect the simplicity advantage of the GaN-based designs, given by the fact that the PFC stages in the GaN-based designs are operated with CCM modulation. This modulation type requires less control and measuring effort than the implementation of TCM modulation with its necessity to detect zero-current switching (ZCS) events.

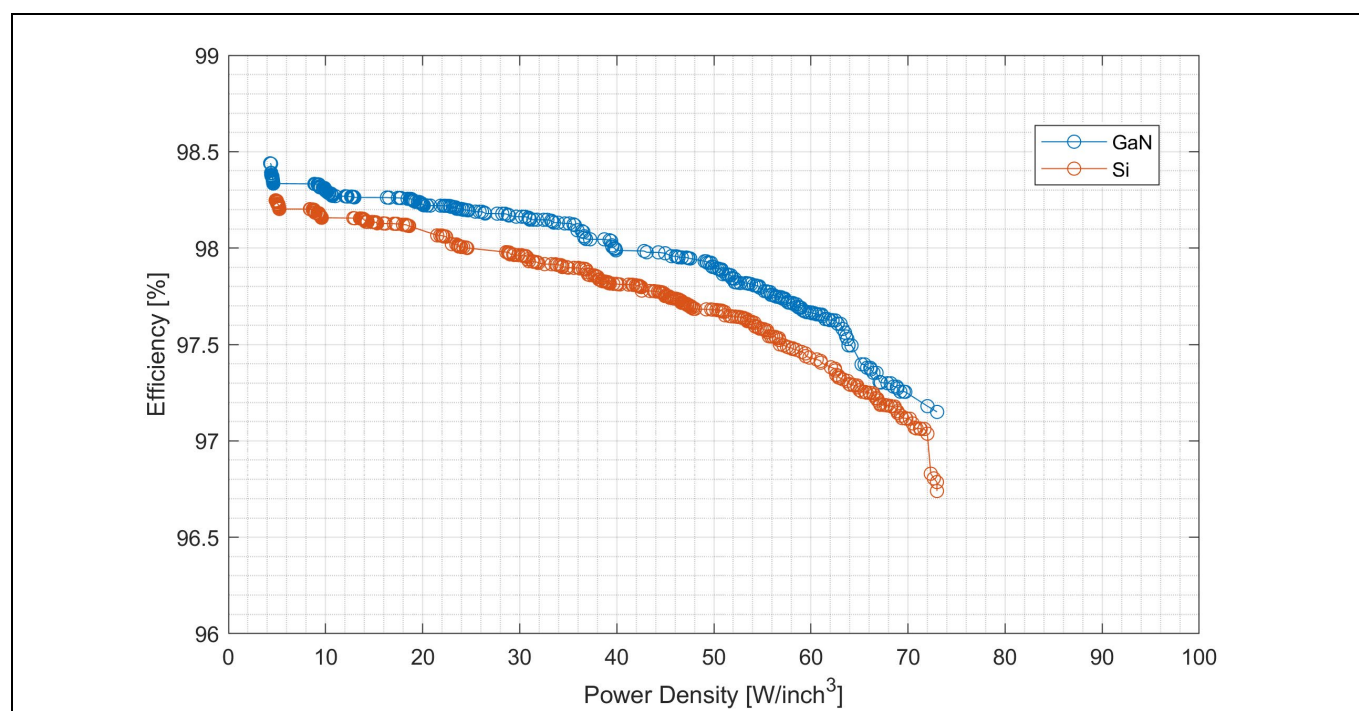


**Figure 14** Pareto-front of the entire 48 V, 3 kW telecom power supply using either GaN- or silicon-based HV devices for 230 V AC<sub>in</sub> and 48 V DC<sub>out</sub>, optimized for 50 percent of the rated power.

The result shows a clear system benefit for GaN-based solutions with an efficiency benefit in the range of 0.3 percent at significantly reduced complexity. Especially the PFC stage will run with GaN devices at fixed frequency using CCM modulation with typically relatively high AC ripple to facilitate natural ZVS switching at least partly across the sinusoidally varying input voltage and different load conditions.

Figure 15 below shows the calculated efficiency of a 3 kW totem-pole PFC stage of a telecom rectifier using CoolGaN™ (in CCM), and CoolMOS™ SJ (in TCM) in the same range of  $R_{DS(on)}$  and running at a comparable switching frequency. The rectifier is supposed to work at the nominal conditions ( $V_{IN} = 230$  V<sub>AC</sub> and  $T_{AMB} = 40^{\circ}\text{C}$ ).



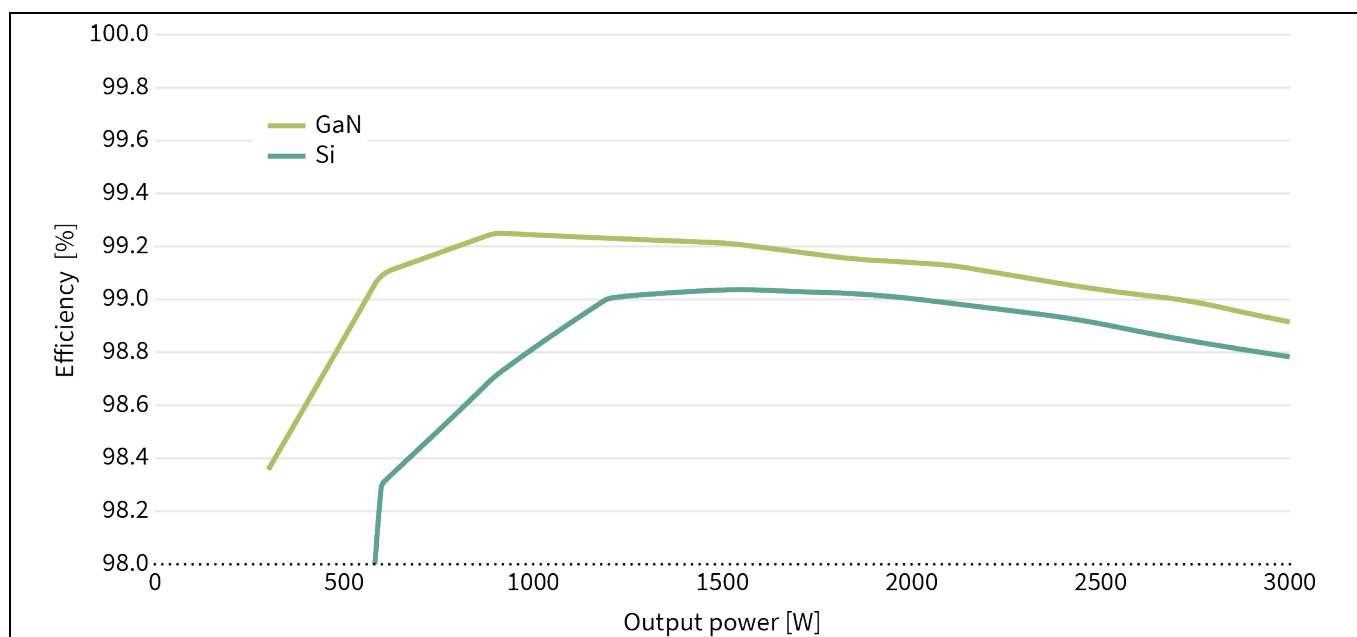


**Figure 15** Calculated efficiency of a 3 kW totem-pole PFC stage of a telecom rectifier using CoolGaN™ (in CCM) and CoolMOS™ SJ (in TCM) in the same range of  $R_{DS(on)}$  and running at a comparable switching frequency

This plot shows that both technologies allow exceeding 99 percent efficiency at 50 percent load. GaN technology shows significant benefits compared to Si SJ below 30 percent load. This is due to the best figures of merit (FOM)  $R_{DS(on)} \cdot Q_{rr}$ ,  $R_{DS(on)} \cdot E_{OSS}$ ,  $R_{DS(on)} \cdot Q_g$ , and  $R_{DS(on)} \cdot Q_{OSS}$  exhibited by the GaN device, as explained in [1,3]. In the load range, which is more in the focus of 5G telecom rectifiers (30-100 percent), we observe a substantially comparable efficiency provided by GaN.

One of the main differences of the Pareto optimal designs in the commercially interesting range of 30...40 W/inch<sup>3</sup> between Si and GaN lies in the PFC stage. The TCM modulation of Si leads to high current ripples and RMS-values of the boost inductor currents. This mandates the interleaving of two HF totem-pole branches to reduce the input current ripple and facilitate a reduced EMI filter size. In contrast, for the CCM-controlled GaN PFC stages, designs with only one HF totem-pole leg are feasible and more cost-effective on the system level due to, e.g., savings in magnetic components.

In the LLC stage, the GaN GIT HEMT-based designs require a lower magnetizing current for soft switching and need shorter delay times. Alternatively, for the same magnetizing current, more parallel GaN switches can be employed in the system. Both alternatives allow reducing the losses in the LLC stage with GaN. The optimization shows that both Si-based and GaN-based designs benefit from a two-stage matrix transformer configuration with primary windings being series-connected and secondary windings being paralleled. Furthermore, full-bridge (FB) rectification yields better results than center-tapped configurations. Switching frequencies are typically around 100 kHz for Si-based designs versus 150 kHz for GaN-based designs.

### 3.2.1 Secondary-side GaN SG HEMTs in the LLC for ultra-high power densities

In systems operating with an output voltage up to 60 V, i.e., telecom and/or server power supplies, an additional option for improving the system performance is offered by employing 100 V Schottky Gate (SG) GaN HEMTs on the secondary side of the LLC. An optimization methodology is also applied by varying the primary side between different Si and GaN technologies, while the secondary side is always a Si synchronous rectifier (SR). In addition to these, a fourth option employing an all-GaN LLC (GaN both on the primary and secondary sides) is considered.

As shown in Figure 16, the selection of GaN on the primary side outperforms an all-silicon LLC by 0.2 to 0.3 percent, depending on the power density. The all-GaN power supply achieves an additional gain in efficiency of 0.2 to 0.3 percent compared to a power supply with GaN only on the primary side. Furthermore, the maximum power density of the all-GaN supplies is around 10 percent higher than the next best GaN with Si synchronous rectifier (SR) alternative. This is because the charge of the GaN SG HEMT 100 V device is considerably lower than that of the Si counterparts. This attribute facilitates the design of smaller resonant tanks with less circulating current as less current is required to change the polarity of the secondary side.

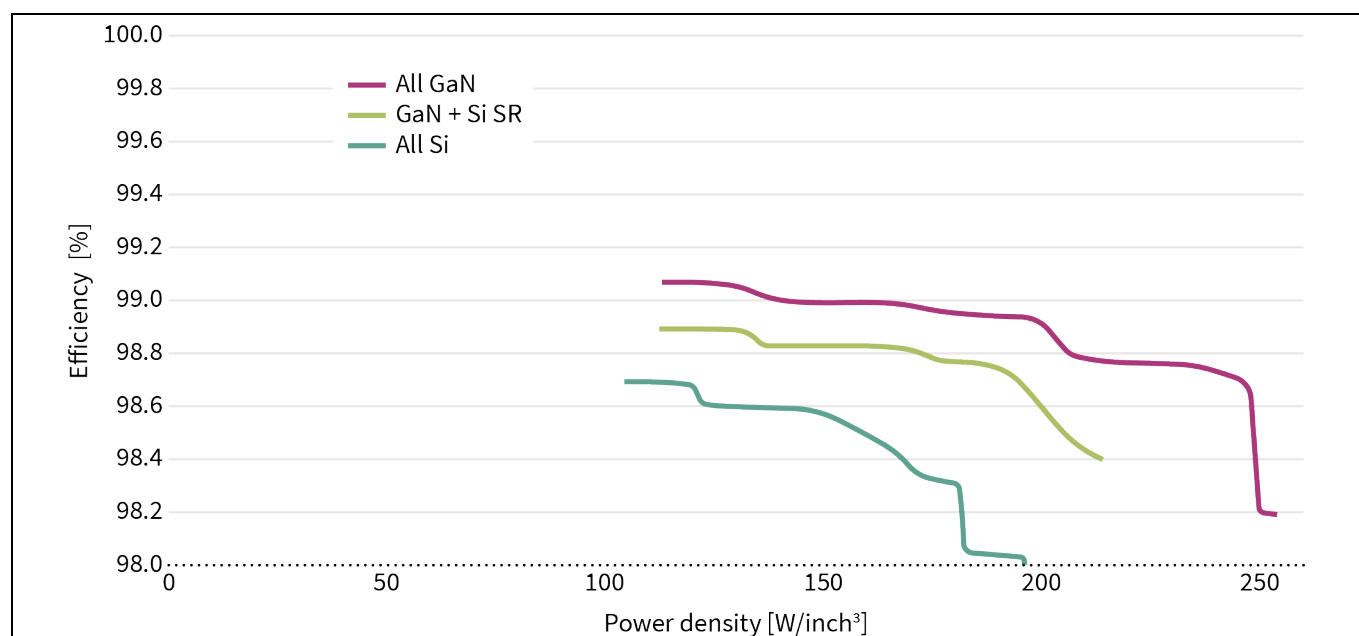


**Figure 16 Optimization results for the LLC stage, showing efficiency versus power density for Si- and GaN-based power devices**

With resonant switching frequencies around 100 kHz, the inevitable (relatively long) dead times of modern SJ devices are not yet limiting and do not lead to a substantial increase of RMS currents. However, when the power density approaches 70 W/inch<sup>3</sup> or more, and the LLC converter's resonant frequency is designed to 300 kHz and beyond, GaN SG HEMTs create clear value. The key argument favoring wide-bandgap devices is their lower  $R_{DS(on)} \cdot Q_{OSS}$  FOM enabling shorter dead times. Also, control schemes such as 3-level modulation, which effectively limit the LLC's frequency range, induce hard commutation transitions, especially during a light load operation. In this case, a very low or even zero  $Q_{rr}$

is an advantage. At very high switching frequencies such as 600 kHz and higher, planar magnetics become a favorable design option as they create even lower losses than conventionally wound transformers.

In this design space, GaN technology is clearly the preferred choice due to its better dynamic figure-of-merits and significantly lower gate charge.

The choice of devices for synchronous rectification depends mainly on the switching frequency. During the secondary side switching transition from a (synchronously) conducting state to blocking, the  $Q_{rr}$  charge creates additional losses, whereas the charging and discharging of the output capacitance is basically loss-less as long as lumped resistances in series with the output capacitance are negligible. Hence, the use of, e.g., 100 V-rated GaN SG HEMTs with their zero  $Q_{rr}$  creates a significant benefit when used as a synchronous rectification switch.

Figure 17 shows the comparison of OptiMOS™ 5 to CoolGaN™ in an LLC converter delivering 3.6 kW at 52 V output. The design uses two secondary-side paralleled stages in full-bridge configuration, with two devices being paralleled in each position. The converter runs at 270 kHz with 97.9 percent peak efficiency using silicon devices and at 340 kHz at 98.5 percent peak efficiency with CoolGaN™ SG HEMTs.

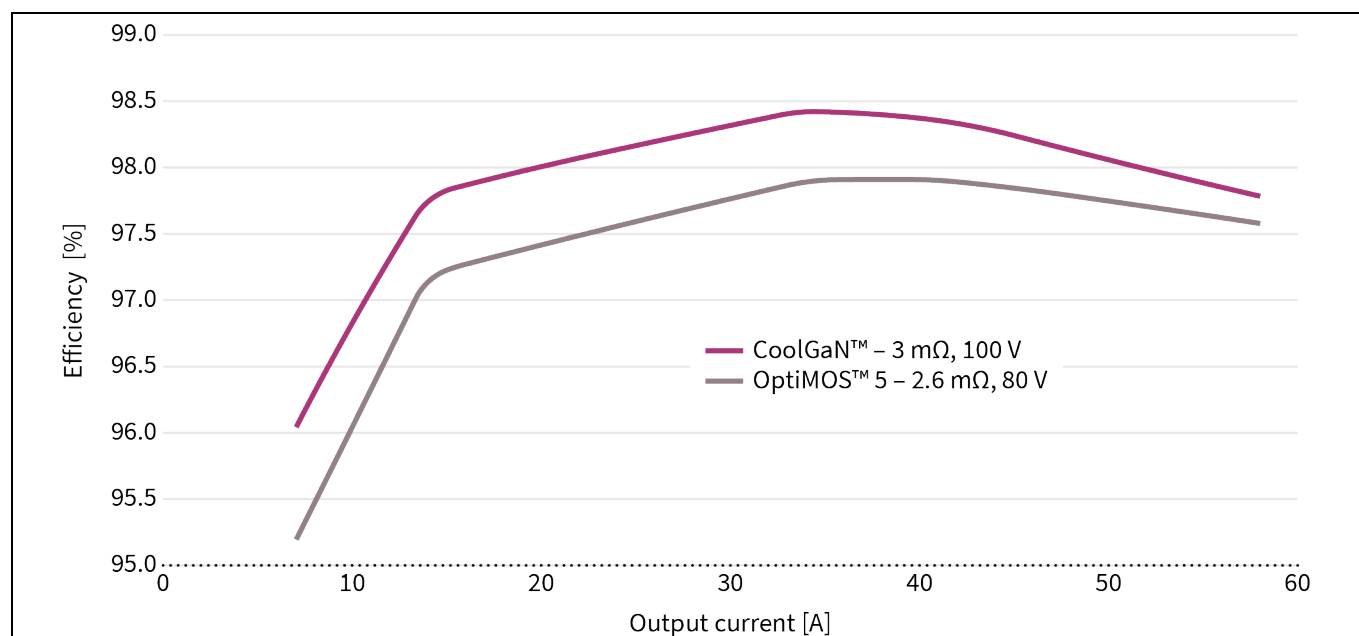


**Figure 17 Efficiency comparison of 100 V-rated CoolGaN™ SG HEMT versus 80 V OptiMOS™ 5 devices used as synchronous rectification switch in a 3.6 kW LLC converter**

## 4 Summary

The application studies performed show a clear value for e-mode GaN HEMTs in high power designs. GaN HEMTs allow us to push both efficiency and density frontiers.

This paper demonstrates a path towards a 98.5 percent efficiency in 48 V servers and a power density of up to 100 W/inch<sup>3</sup> for 12 V servers, thus offering significant benefits in terms of OPEX and CAPEX savings. It also shows that GaN allows using less complex control schemes such as CCM modulation in the PFC stage due to its hard switching capabilities while at the same time offering performance benefits compared to the next best Si alternative. Furthermore, the performance benefit of medium voltage GaN components for synchronous rectification in the LLC stage has been shown.

Compared to their silicon counterparts, the attractiveness of GaN-based technologies depends mainly on the application's requirements concerning efficiency and power density, which guide the designers towards choosing the best-fitting device technology. On this basis, the optimization results manifest the design superiority when using GaN-based power devices over silicon in terms of efficiency versus power density. Also, they highlight the necessary design trade-offs that indicate the appropriate choices.

To learn more about Infineon's CoolGaN™ portfolio of power switches and dedicated GaN-optimized EiceDRIVER™ driver ICs, please visit [www.infineon.com/gan](http://www.infineon.com/gan) and [www.infineon.com/gan-eicedriver](http://www.infineon.com/gan-eicedriver), respectively.

## References

- [1] M. Kasper, D. Bortis, G. Deboy, and J. W. Kolar, "Design of a Highly Efficient (97.7%) and Very Compact (2.2 kW/dm<sup>3</sup>) Isolated AC–DC Telecom Power Supply Module Based on the Multicell ISOP Converter Approach," in *IEEE Transactions on Power Electronics*, vol. 32, no. 10, pp. 7750-7769, Oct. 2017
- [2] F. Udrea, G. Deboy and T. Fujihira, "Superjunction Power devices, History, Development and Future prospects," *Transactions on Electron Devices*, Vol. 64, No. 3, March 2017, pp. 713-727
- [3] G. Deboy, O. Haeberlen, and M. Treu, "Perspective of loss mechanisms for silicon and wide-bandgap power devices," *CPSS Transactions on Power electronics and applications*, Vol. 2, No. 2, June 2017, pp. 89-100
- [4] D. Neumayr, D. Bortis, E. Hatipoglu, J. W. Kolar and G. Deboy, "Novel efficiency-Optimal Frequency Modulation for high power density DC/AC converter systems," 2017 IEEE 3rd International Future Energy Electronics Conference and ECCE Asia (IFEEEC 2017 - ECCE Asia), Kaohsiung, 2017, pp. 834-839



[www.infineon.com](http://www.infineon.com)

Published by  
Infineon Technologies AG  
Am Campeon 1-15, 85579 Neubiberg  
Germany

© 2022 Infineon Technologies AG.  
All rights reserved.

Document number: B152-I0733-V1-7600-EU-EC  
Date: 02 / 2022

#### **Please note!**

This Document is for information purposes only and any information given herein shall in no event be regarded as a warranty, guarantee or description of any functionality, conditions and/or quality of our products or any suitability for a particular purpose. With regard to the technical specifications of our products, we kindly ask you to refer to the relevant product data sheets provided by us. Our customers and their technical departments are required to evaluate the suitability of our products for the intended application.

We reserve the right to change this document and/or the information given herein at any time.

#### **Additional information**

For further information on technologies, our products, the application of our products, delivery terms and conditions and/or prices please contact your nearest Infineon Technologies office ([www.infineon.com](http://www.infineon.com)).

#### **Warnings**

Due to technical requirements, our products may contain dangerous substances. For information on the types in question, please contact your nearest Infineon Technologies office.

Except as otherwise explicitly approved by us in a written document signed by authorized representatives of Infineon Technologies, our products may not be used in any life-endangering applications, including but not limited to medical, nuclear, military, life-critical or any other applications where a failure of the product or any consequences of the use thereof can result in personal injury.